Available online at www.sciencedirect.com
ScienceDirect
Applied Catalysis A: General 329 (2007) 130–136
APPLIED CATALYSIS A: GENERAL
www.elsevier.com/locate/apcata

Methanol conversion on SAPO-34 catalysts prepared by mixed template method

Yun-Jo Lee, Seung-Chan Baek, Ki-Won Jun *

Alternative Chemicals/Fuel Research Center, Korea Research Institute of Chemical Technology, P.O. Box 107, Yuseong, Daejeon 305-600, South Korea

Received 18 December 2006; received in revised form 25 May 2007; accepted 4 June 2007
Available online 7 July 2007

Abstract

Effects of templating on the catalytic performance of SAPO-34 catalyst have been investigated in conversion of methanol to olefins (MTO). SAPO-34 catalysts were synthesized using a single agent or a mixture of morpholine or tetraethyl ammonium hydroxide of (TEAOH) as the template during synthesis of gel with nominal composition as $1Al_2O_3$:$1P_2O_5$:$0.6SiO_2$:x morpholine:$(2-x)$TEAOH:$52H_2O$. Compared with using single template, using a mixed template leads to the particle size reduction and the morphology change to spherical type formed by the aggregation of nano-sized crystals. Although all the catalysts showed similar activity and product distribution in the MTO reaction, the catalyst obtained using the mixture of 75% morpholine and 25% TEAOH gave the longest lifetime.

Keywords: MTO; SAPO-34; Mixed template; Methanol; Olefins

1. Introduction

Small pore silicoaluminophosphate molecular sieve, SAPO-34 is well known to be one of the best catalysts in the conversion of methanol to olefins (MTO) [1–6]. It gives a very high selectivity (>80%) to light olefins (C_2–C_4) with almost 100% conversion of methanol, which is mainly attributed to its mild acidity and shape selective catalysis by small pore entrance. However, the main problem associated with these catalysts is rapid deactivation of SAPO-34 due to coke formation during MTO reaction [7–11] and this resultantly makes the lifetime of these catalysts short. Although the catalysts are regenerated by hot-air blowing, loss of carbon can not be avoided. Therefore, it is necessary to develop the catalysts which are more resistant to coke formation. Considering these facts, in the present work, SAPO-34 catalysts were prepared with mixed templating agents and their catalytic activity, selectivity and stability were examined in the MTO reaction. The performance parameter of SAPO-34 catalysts, namely catalyst stability was found to be affected by the preparation parameters during synthesis which are closely related with crystal size and the silicon contents during synthesis. All of these results related to synthesis and characterization are presented in this paper.

2. Experimental

2.1. Catalyst preparation

The silicoaluminophosphate (SAPO) molecular sieve catalysts were synthesized hydrothermally using the mixtures of morpholine and tetraethylammonium hydroxide (TEAOH) as templating agent via a suitable modification of the reported method [12]. The molar composition for synthesis of the catalysts was kept as $1.0Al_2O_3$:$1.0P_2O_5$:$0.6SiO_2$:x morpholine:$(2.0-x)$TEAOH: $52H_2O$ (x = 2.0, 1.8, 1.5, 1.0, 0.5, 0.0). The synthesis procedure followed for gel preparation in typical experiment with x = 1.0 is described as given below.

14.16 g of pseudoboehmite (catapal A, 74.2% Al_2O_3, Vista chemicals) was added to 25 mL of water, and then mixture of 23.06 g of phosphoric acid (85%, Samchun chemicals) and 1.8 mL of water was added to the alumina solution under stirring by a drop-wise addition for 2 h and then the resulting solution was stirred for 2 h at room temperature. Clear silica solution was further added, which was prepared by dissolution

* Corresponding author.
E-mail address: kwjun@krict.re.kr (K.-W. Jun).

0926-860X/$ – see front matter
doi:10.1016/j.apcata.2007.06.034

of 9.01 g of colloidal silica (Ludox As-40, 40% SiO_2) into 42.09 g of 35% TEAOH aqueous solution (Aldrich) at 100 °C for 12 h by stirring. Finally, 8.71 g of morpholine (Aldrich) and 12 mL of water was added and the resulting mixture was stirred for 25 h. The resulting gel mass was transferred into autoclave and heated in two steps of 120 and 200 °C and maintained for 12 h at each temperature with vigorous stirring. The solid product was recovered by centrifugation, washed several times with distilled water and dried overnight at 120 °C. As-synthesized product was then calcined in air at 550 °C.

2.2. Characterization

The powder X-ray diffraction (XRD) patterns of as-synthesized catalysts were obtained on a Rigaku D/MAX IIIB X-ray diffractometer with Cu Kα radiations. The morphology of the samples was observed using a scanning electron microscope (Philips XL 30S FEG microscope). The surface acidity of the catalysts was measured by temperature programmed desorption of ammonia (NH_3-TPD) using a BEL-CAT TPD analyzer with TCD detector. In a typical analysis, 0.2 g of the calcined sample was pretreated to remove adsorbed water at 500 °C for 3 h and then saturated with ammonia at 100 °C for 1 h. After saturation, the sample was purged with helium for 30 min to remove the weakly adsorbed ammonia on the surface of the catalyst. The temperature of the sample was then raised at a heating rate 10 °C/min from 100 to 700 °C. The amount of ammonia desorbed from the catalyst was measured by comparing the TPD areas with that for standard sample. Thermo-gravimetric analysis (TGA) and differential thermal analysis (DTA) were performed to detect the thermal decomposition of amine templates of as-synthesized catalysts using TA Instrument (DMA, SDT 2960) under an air flow (100 mL/min) at a heating rate of 10 °C/min from room temperature up to 800 °C. The BET surface areas of calcined samples were determined from isotherm data of nitrogen adsorption–desorption obtained at −196 °C using Micromeritics ASAP-2400 analyzer. Elemental analysis for Al, P and Si of calcined samples was done by inductively coupled plasma atomic emission spectrometry (ICP-AES, ULTIMC, Jobin Yvon Inc.) after dissolving the samples into 1N HNO_3 solution.

2.3. Catalytic reaction

The conversion reactions of methanol to olefins were carried out in a fixed bed down flow micro-reactor and at atmospheric pressure and in the temperature range of 250–500 °C. A known weight (0.489 g) of calcined SAPO catalyst (20–50 mesh) was packed in the center of stainless steel (i.d.: 1 cm, length: 30 cm) reactor and heated by a tubular furnace. Methanol with a liquid flow rate of 0.01 mL/min was fed by syringe pump into a preheater kept at 300 °C. Helium was used as an inert diluent gas and co-fed with methanol into the reactor at a flow rate of 60 mL/min and the ratio of methanol: He was maintained to 1:10.89 in vol.%, where space velocity in WHSV was kept to 1 h^{-1}. The analysis of the reaction products was performed using an on-line gas chromatograph (Donam GC 6100) equipped with flame ionization (FID) and thermal conductivity (TCD) detector with Gas-Pro and Plot-Q capillary columns for hydrocarbons and oxygenates, respectively.

3. Result and discussions

3.1. Characterization

Fig. 1 shows X-ray diffraction patterns of as-synthesized SAPO samples prepared by mixed template method. Fig. 1(a–d) shows typical powder diffraction patterns corresponding to CHA-structure of SAPO-34 where intensity and peak position of each peak match well with that of reported for SAPO-34 material without any presence of impurity phases [13]. However, with increase of TEAOH ratio from 0 to 1.5, a decrease in peak intensity and line broadening is observed as is seen from Fig. 1(a–d). Based on XRD peak intensity of peak appearing at $2\theta = 22.5°$, the crystallinity of SAPO-34 phase is determined and found to be 71.6%, 48.4% and 25.1%, respectively.

When TEAOH is only used as a template agent without using morpholine, the crystalline phase of as synthesized sample is found to be significantly different as is seen in Fig. 1(e). Major product is SAPO-5 (92%) with presence of minor one, i.e. SAPO-34 (8%). Although the TEAOH is a good template agent for the synthesis of SAPO-34 [14], SAPO-5 instead of SAPO-34 is obtained as a major crystal phase due to high Si content and/or our existing experimental conditions [15]. It was also observed that the reduction in Si content during synthesis of gel to half under the same synthesis conditions led to the formation of only pure SAPO-34 phase. Table 1 presents the summary of preparation conditions and phase data, based on the XRD results, of the SAPO samples prepared using mixed template.

The results of ICP-AES analyses and surface area data are given in Table 2 for the as-synthesized samples. Compared to Si/(Al + P + Si) = 0.130 for all starting gels, the ratio of the product samples was found to be higher than 0.146 after crystallization, which means more amounts of Si was incorporated into the framework of SAPO molecular sieves and/or remained as amorphous silica phase on extra-framework. The Si content in

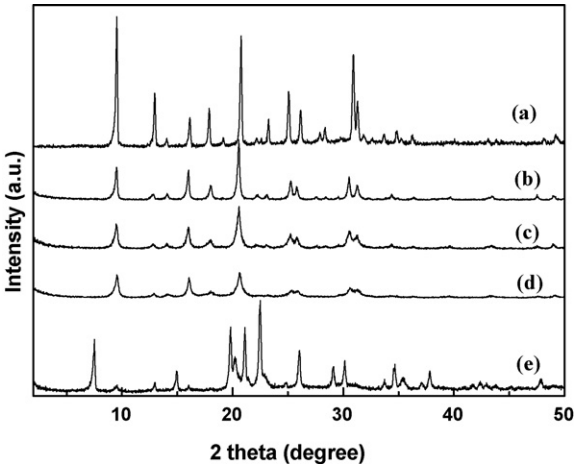

Fig. 1. XRD patterns of as-synthesized SAPO samples: (a) M20, (b) M15, (c) M10, (d) M5 and (e) M0.

Table 1
Preparation conditions for SAPO-34 samples and their confirmed phase

Samples	Gel composition[a] (x)	Temperature (°C)	Time (h)	Product phase
M20	2.0	200	12	SAPO-34
M15	1.5	200	12	SAPO-34
M10	1.0	200	12	SAPO-34
M5	0.5	200	12	SAPO-34
M0	0	200	12	SAPO-5 (92%) + SAPO-34 (8%)

[a] $1.0Al_2O_3$:$1.0P_2O_5$:$0.6SiO_2$:x morpholine:$(2-x)$TEAOH:$52H_2O$, where x is defined as the mole ratio of morpholine to alumina.

Table 2
Physicochemical properties of synthesized SAPO catalysts

Samples	Elemental analysis[a]			BET surface area (m^2/g)	Amount of desorbed ammonia (mmol/g)[b]	
	Al	P	Si		200 °C	430 °C
M20	0.448	0.405	0.146	772	0.35	0.62
M15	0.443	0.388	0.169	728	0.43	0.60
M10	0.433	0.391	0.175	665	0.43	0.59
M5	0.437	0.386	0.177	623	0.34	0.33
M0	0.442	0.390	0.179	284	0.28[c]	–

[a] Analyzed by ICP-AES.
[b] Analyzed by NH_3-TPD.
[c] Total amount.

the product samples also gradually increases with increase of TEAOH content in the synthesis gel. When we compare the XRD data of Fig. 1, it is clear that the parts of Si most probably remain in extra-framework as amorphous phase in M15, M10, and M5 samples and this inference was confirmed by NH_3 TPD data, which is discussed later in detail. M20 sample synthesized without TEAOH showed lowest and steep decrease in Si content compared to other TEAOH containing samples.

Table 2 also shows the BET surface area data of the samples measured by nitrogen adsorption–desorption experiment. The surface area decreased from 772 to 284 m^2/g when TEAOH content increased from $x = 0$ to $x = 2.0$ during the synthesis of gel. Gradual decrease in the surface area was observed in the range of TEAOH from $x = 0$ to $x = 1.5$. This observation strongly suggests that the sample partially lost its crystallinity, and it became amorphous with increasing TEAOH. This observation is consistent with XRD results discussed earlier where crystallinity is found to be decreased with increasing TEAOH ratio. The steep decrease in surface area was observed in the sample (M0) when x is changed from 1.5 to 2.0 in TEAOH content. This may be possibly be related to the change in crystal phase from CHA- to AFI-type molecular sieve. Generally CHA-type molecular sieve has larger BET surface area than ones with AFI [16].

Fig. 2 shows SEM images for as-synthesized samples. M20 sample in Fig. 2(a) exhibits the rhombohedral shape of typical SAPO-34 with average particle size of 5–20 μm, which is typical when morpholine is used as a template agent [17]. M15

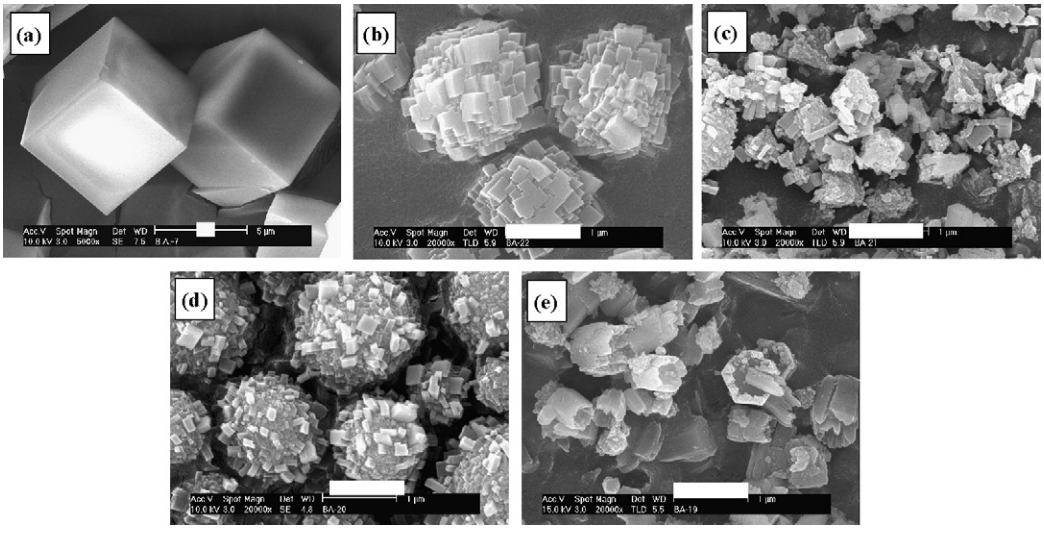

Fig. 2. SEM images of the prepared SAPO samples: (a) M20, (b) M15, (c) M10, (d) M5 and (e) M0. Bars correspond to 1 μm.

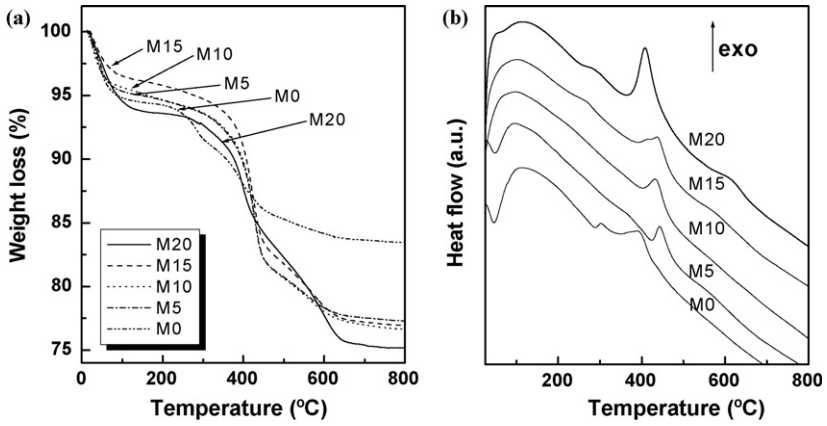

Fig. 3. TGA (a) and DTA (b) curves of as-synthesized SAPO samples.

sample, however, shows spherical aggregates of nano-sized cube type SAPO-34 crystals where the aggregates showed average crystal size of 1 μm with homogeneous size distribution. M10 as-synthesized sample (with morpholine and TEAOH in equal amounts) shows irregular shape in morphology with crystal size in sub-micrometer range. The M5 sample shows very interesting morphology where the surface of spherical shaped particle was aggregated with SAPO-34 nanocrystals. On the other hand, M0 sample shows hexagonal type crystal habit which is typical SAPO-5 morphology. Thus, the SEM study confirms that morphology of the final product is dependent on the nature of template used during synthesis.

Fig. 3 shows TGA/DTA curves for all the synthesized samples. TGA/DTA results for M20, M15, M10 and M5 samples showed similar weight loss pattern in the temperature ranges of 25–100, 100–450 and 450–800 °C. The first weight loss, accompanied with endothermic peak appearing in DTA curve, is attributable to the physically adsorbed water associated with SAPO samples. The second weight loss in TGA curve centered at around 410–460 °C, accompanied with strong exothermic DTA peak, is attributed to the oxidative decomposition of organic templates. The third weight loss in TGA curve centered at around 550 °C, accompanied with weak broad exothermic DTA peak, may be related to the oxidation of organic templates also. The third weight loss increased gradually with increase of morpholine content in the samples from sample M5 to M20, which is related due to the loss of template trapped at ion-exchange site within CHA cage of SAPO-34 [17]. M0 sample synthesized using TEAOH only, which showed a major phase of SAPO-5, exhibited weight losses in three stages. The first stage is assigned to the desorption of water and the second stage with endothermic peak at around 300 °C to the desorption of TEAOH and the last at temperature ranged from 370 to 800 °C is attributed to the oxidative decomposition of TEAOH in the sample. The TGA/DTA study indicated that complete decomposition of template occurs at temperatures greater than 550 °C hence the calcination was carried at the said temperature during the present investigation.

TPD of ammonia was used to characterize the acidic properties of SAPO samples and curves obtained for the same are shown in Fig. 4. Two TPD peaks for SAPO-34 samples at temperatures 200 and 430 °C were observed. They are in accordance with the reported literature data for the acidity of SAPO materials [18]. Total ammonia amount desorbed are narrowly ranged to ca. 1.0 mmol/g for the SAPO-34 samples. The intensity of high temperature desorption peak appearing at 430 °C assigned to the strong acidic sites which are generated by the incorporation of silicon into the framework of SAPO molecular sieve, decreased with increase of TEAOH in the order of M20 > M15 > M10 > M5 > M0. Low temperature peak at ca. 200 °C, assigned to the weak acid sites which are probably Brönsted acid sites originating from P-OH groups not fully linked to AlO_4 tetrahedra [18], showed no apparent difference in peak intensity with TEAOH amounts. Peak intensity of high temperature desorption peak decreased with increase of TEAOH amount whereas Si content in product samples increased with TEAOH amount as shown in ICP-AES results of Table 2, which means that some part of Si in M15, M10 and M5 samples could exist as amorphous silica in extra-framework of SAPO samples and its amount could also be increased in proportion to TEAOH amount. This observation is also supported by XRD data in Fig. 1, where it exhibited gradual decrease in XRD peak intensity for SAPO-34 with higher TEAOH amount. Fig. 4(e) shows NH_3-TPD pattern for M0 sample. A very weak desorption peak in high temperature

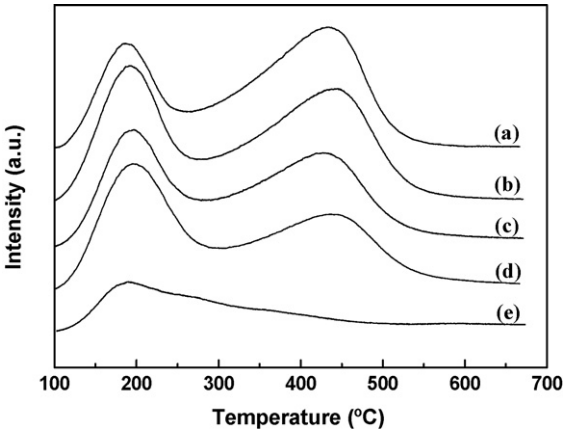

Fig. 4. NH_3-TPD profiles for the calcined SAPO catalysts: (a) M20, (b) M15, (c) M10, (d) M5 and (e) M0.

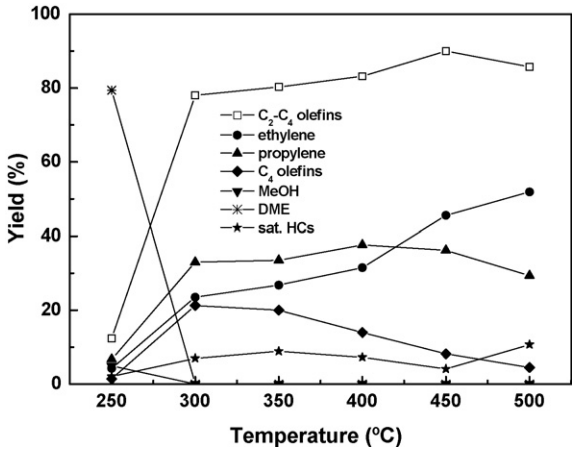

Fig. 5. Effect of reaction temperature on methanol conversion and product distribution. Feed: MeOH/He = 1/11 (molar ratio), WHSV(MeOH) = 1 h^{-1}, time on stream = 1 h.

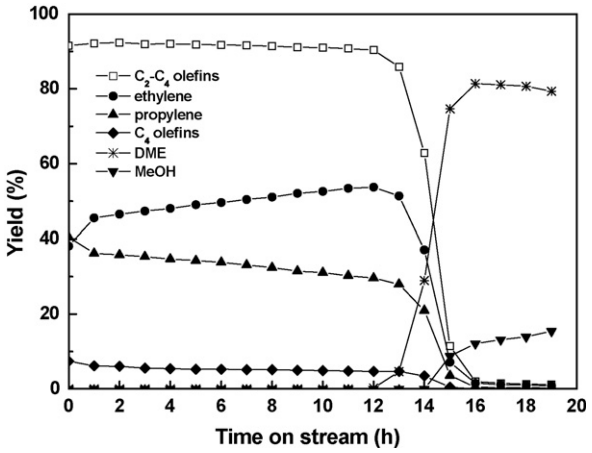

Fig. 6. Product distribution with time-on-stream over M15 catalyst. Feed: MeOH/He = 1/11 (molar ratio), WHSV(MeOH) = 1 h^{-1}.

region compared to SAPO-34 samples and strong peak at low acidity region were observed, which is similar to typical ones of SAPO-5 sample reported in literature [19].

3.2. Activity test for MTO reaction

Fig. 5 shows the product distribution for methanol conversion reaction on M15 sample as a function reaction temperature. For every reaction temperature, the fresh catalyst was loaded to collect the reaction data. The measurements of yield of reaction products in Fig. 5 correspond to a time-on-stream (TOS) of 1 h at each temperature. At 250 °C methanol was converted mostly to dimethylether (DME) with ca. 80% yield as an intermediate product. As the temperature increased from 300 to 500 °C, the MeOH conversion became complete and yield of light olefins (ethylene, propylene and butenes) was significant and became more than 80%, whereas yield of saturated hydrocarbon was maintained less than 10% in whole reaction temperature. With further increase of reaction temperature, C_4 olefins gave maximum value of about 20% at 300 °C, which gradually decreased with increasing temperature. In the case of propylene, the yield increased with increasing temperature up to 400 °C afterward decreased at 500 °C, whereas yield of ethylene steadily increased in the whole reaction temperature. The reason for this phenomenon is that propylene and butenes can oligomerize to bigger oligomers, which crack to form ethylene at higher temperature. That is why yields of propylene and butenes have maximum values at low or medium temperature, while the yield of ethylene steadily increases with reaction temperature. The ethylene to propylene molar ratio increased from 0.71 at 300 °C to 1.77 at 500 °C. Yield of olefins has maximum value at 450 °C and decreases at 500 °C with increase of yield of saturated hydrocarbon (mainly, methane).

Fig. 6 shows the yield of products with TOS on M15 at 450 °C. The yield of light olefins was maintained over 90% until catalytic activity abruptly decreased by deactivation of catalyst. Catalyst deactivation on MTO reaction would mainly be preceded by coke formation. The coke would cover acidic sites and also block the pore of SAPO-34. SAPO-34 has CHA cage (7.5 Å × 8.2 Å) enough to accommodate coke or coke precursor.

Before catalyst deactivation the yield of ethylene increased with TOS and accompanied the concomitant decrease of propylene. The DME yield in the product steeply increased with start of catalyst deactivation and reached a maximum of 80%. DME as a reaction intermediate can easily be converted to olefins in acidic sites until the cages are occupied by coke. Once the cages are occupied by coke, yield of olefins is abruptly decreased [2]. However, even after deactivation of the catalyst in reaction of methanol to olefins, conversion reaction of methanol to DME can take place on the weak acidic sites of external surface of SAPO-34 because this reaction can occur at weaker acidic sites than the reaction of methanol to olefins. The ethylene to propylene ratio reached a maximum of 1.81 just before the deactivation, namely at 12 h of TOS.

Table 3 gives product distribution and lifetime of catalysts on all the SAPO samples, which was measured in 1 h of TOS at 450 °C. All these catalysts had complete conversion of methanol and mostly conversion to light olefins. When the reaction was conducted to give partial conversion (84%) at much lower temperature of 250 °C, yield of DME was 69.6% while total yield of C_2–C_4 olefins was merely 12.4%. Since the comparison of selectivity of each sample in low conversion of methanol would give mainly information about DME formation but little information about olefin formation, we present the data of product distribution under the condition which gives mainly olefins production. M20 catalyst, synthesized with morpholine only, shows shortest catalyst lifetime (here we defined 'catalyst lifetime' as time sustaining catalyst activity until total yield of C_2–C_4 olefins exceeds 70%) and high yield in saturated hydrocarbons. These results may be explained by crystal size of M20 catalyst. Big crystal can bring diffusion limitation for reactants and products especially in small pore molecular sieve, which may result in coke formation and subsequently deactivation of the catalyst [20]. Big crystal has long intracrystalline diffusion length enough for the reaction intermediates to react into coke which subsequently deactivate the catalyst. On the other hand, when the big crystals of M20

Table 3
Product distribution and catalyst lifetime on SAPO catalysts in methanol conversion reaction[a]

Samples	Catalyst lifetime (min)	MeOH conversion (%)	Product yields (%)			
			C_2^{2-}	C_3^{2-}	C_4^{2-}	Saturated HCs
M20	160	100	42.8	39.1	8.0	10.2
M15	840	100	45.6	36.2	6.2	4.1
M10	520	100	44.6	37.4	6.6	3.0
M5	430	100	42.4	33.9	6.2	3.3
M0	370	100	19.9	40.3	16.0	5.5

[a] Catalyst = 0.49 g of H-SAPO-34, WHSV(MeOH) = 1 h^{-1}, MeOH:He = 1:11(mol/mol), reaction temperature = 450 °C.

sample were crushed into smaller crystals of about 1 μm by ball milling, the lifetime of the catalyst increased with more than three times compared with that of original sample. This supports that catalyst lifetime strongly depends on crystal size of SAPO-34. The strong acidity of M20 catalyst associated with big crystal size promoted hydrogen transfer reaction of olefins to saturated hydrocarbons and aromatics, which are precursors of coke formation. The catalysts, e.g. M15, M10 and M5 showed very similar product distributions with high yield in light olefins. However, there was large difference in catalyst lifetime. The M15 catalyst maintained activity for 840 min until total yield of C_2–C_4 olefins maintains upper 70% (see Fig. 7). The lifetime was in order of M15 > M10 > M5 > M0 > M20. Crystal size of the samples decreases in order of M20 > M15 > M10 as shown in SEM images of Fig. 2. We can see that M5 sample consists of spheres of about 1 μm aggregated with nanocrystals as shown in SEM images. This is also supported by the broadness of XRD peaks in M5 sample. Therefore, genuine crystal size decreases in order of M20 > M15 > M10 > M5. In the case of M10 and M5 samples, they have too short diffusion length for reaction intermediate to react to olefins. Thus longest lifetime of M15 with optimum crystal size of about 1 μm can be explained by crystal size effect because M20, M15, M10 and M5 samples have similar acidic properties (Fig. 2, Table 2) and same crystal structure of CHA topology.

On the other hand, crystallinity and specific surface area decreased in order of M15 > M10 > M5 which may also be related with the lifetime. M0 catalyst showed different product distribution with relatively high yield in C_4 and C_3 olefins compared to other catalysts. M0 catalyst consists of the mixture of SAPO-5 (92%) and SAPO-34 (8%). The SAPO-5 is large pore molecular sieve with AFI topology where 1-D straight channel consists of the 7.3 Å × 7.3 Å pore entrance. Product molecules in SAPO-5 can be easily escaped in the pore without further reaction. Therefore, the yield of C_3 and C_4 olefins in SAPO-5 was higher as compared to SAPO-34. This result is agreement with that reported in the literature [21].

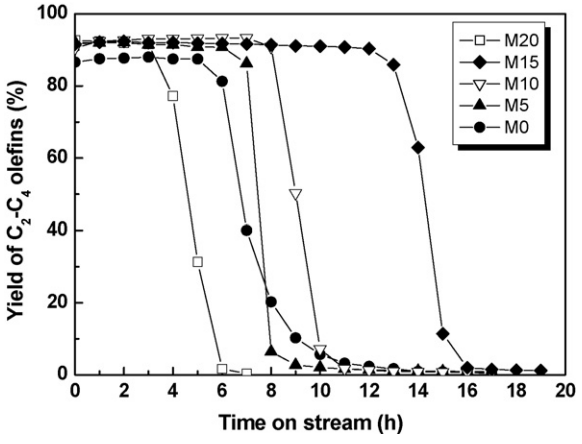

Fig. 7. Yield of C_2–C_4 olefins with time-on-stream over SAPO catalysts. Feed: MeOH/He = 1/11 (molar ratio), WHSV(MeOH) = 1 h^{-1}.

Fig. 7 shows yield of light olefins on TOS in all the catalysts. All the catalysts except for M0 exhibited more than 90% yield in the olefins with abrupt decrease on TOS by catalyst deactivation. Compared with other catalysts, M0 sample showed a slightly lower yield in olefins and a little slow decay in catalyst diminishment which is due to larger pore and lower acidity.

4. Conclusions

The variety in morphology, crystal size and structure of SAPO catalysts can be achieved by using a mixture of morpholine and TEAOH as the template. When the mixture is used for the synthesis of SAPO-34, the crystal size is decreased to sub-micrometer size and the morphology of the crystal is changed to spherical type formed by aggregation of nano-sized crystals. All the prepared SAPO-34 catalysts show similar activity and product distribution in the MTO reaction. However, the catalyst obtained using the mixture of 75% morpholine and 25% TEAOH has the longest lifetime. The lifetime is increased by five times compared to that of the catalyst synthesized with 100% morpholine.

Acknowledgements

This research was supported by a grant (code# CA2-101-1-0-1) from Carbon Dioxide Reduction & Sequestration Center (CDRS), one of 21st Century Frontier Programs funded by the Ministry of Science and Technology, Republic of Korea.

References

[1] M. Stöcker, Microporous Mesoporous Mater. 29 (1999) 3.
[2] A.J. Marchi, G.F. Froment, Appl. Catal. A: Gen. 71 (1991) 139.
[3] T. Inui, H. Matsuda, H. Okaniwa, A. Miyamoto, Appl. Catal. A: Gen. 58 (1990) 155.

[4] Y. Xu, C. Grey, J.M. Thomas, A.K. Cheetham, Catal. Lett. 4 (1990) 251.
[5] M.-A. Djieugoue, A.M. Prakash, L. Kevan, J. Phys. Chem. B 104 (2000) 6452.
[6] J.M. Thomas, Y. Xu, C.R.A. Catlow, J.W. Couves, Chem. Mater. 3 (1991) 661.
[7] J. Liang, H. Li, S. Zhao, W. Guo, R. Wang, M. Ying, Appl. Catal. A: Gen. 64 (1990) 31.
[8] M.J. Van Niekerk, J.C.Q. Fletcher, C.T. O'Connor, Appl. Catal. A: Gen. 138 (1996) 135.
[9] D. Chen, H.P. Rebo, A. Grønvold, K. Moljord, A. Holmen, Microporous Mesoporous Mater. 35–36 (2000) 121.
[10] X. Wu, R.G. Anthony, Appl. Catal. A: Gen. 218 (2001) 241.
[11] D. Chen, H.P. Rebo, K. Moljord, HolmenF A., in: B. Delmon, J.T. Yates (Eds.), Catalyst Deactivation, Studies in Surface Science and Catalysis, vol. 111, Elsevier, Amsterdam, 1997, p. 159.
[12] A.M. Prakash, S. Unnikrishnan, J. Chem. Soc., Faraday Trans. 90 (1994) 2291.
[13] J.J. Pluth, J.V. Smith, J. Phys. Chem. 93 (1989) 6516.
[14] M. Popova, C. Minchev, V. Kanazirev, Appl. Catal. A: Gen. 169 (1998) 227.
[15] S.H. Jhung, J.-S. Chang, J.S. Hwang, S.-E. Park, Microporous Mesoporous Mater. 64 (2003) 33.
[16] S.H. Jhung, J.-H. Lee, J.W. Yoon, J.-S. Hwang, S.-E. Park, J.-S. Chang, Microporous Mesoporous Mater. 80 (2005) 147.
[17] L. Marchese, A. Frache, E. Gianotti, G. Martra, M. Causa, S. Coluccia, Microporous Mesoporous Mater. 30 (1999) 145.
[18] B. Parlitz, E. Schreier, H.-L. Zubowa, R. Eckelt, E. Lieschke, R. Fricke, J. Catal. 155 (1995) 1.
[19] T.-C. Xiao, L.-D. An, H.-L. Wang, Appl. Catal. A: Gen. 130 (1995) 187.
[20] D. Chen, K. Moljord, T. Fuglerud, A. Holmen, Microporous Mesoporous Mater. 29 (1999) 191.
[21] J.M. Campelo, F. Lafont, J.M. Marinas, M. Ojeda, Appl. Catal. A: Gen. 192 (2000) 85.